Current and Strain-Induced Spin Polarization in InGaN/GaN Superlattices

H. J. Chang, T. W. Chen, J. W. Chen, W. C. Hong, W. C. Tsai, Y. F. Chen, and G. Y. Guo

Department of Physics, National Taiwan University, Taipei 106, Taiwan
(Received 2 November 2006; published 28 March 2007)

The lateral current-induced spin polarization in InGaN/GaN superlattices (SLs) without an applied magnetic field is reported. The fact that the sign of the nonequilibrium spin changes as the current reverses and is opposite for the two edges provides a clear signature for the spin Hall effect. In addition, it is discovered that the spin Hall effect can be strongly manipulated by the internal strains. A theoretical work has also been developed to understand the observed strain-induced spin polarization. Our result paves an alternative way for the generation of spin polarized current.

It has been proposed theoretically that a transverse spin current, the so-called spin Hall current, can be generated in strongly spin-orbit coupling systems by an external electric field [1–5]. This novel phenomenon offers the exciting possibility of pure electric driven spintronics in semiconductors, which can be more readily integrated with current industry. Recently, the observations of the spin Hall effect have been reported [6,7] in GaAs based devices, which has generated an intensive research [8–12]. However, up to now, most of the experimental measurements were concentrated on the GaAs system. More clear evidence to confirm the spin Hall effect in other semiconductors is still needed [13]. Nitride semiconductors probably represent the most studied material system in semiconductor community for the last decade. InGaN/GaN superlattices have become particularly attractive because of their wide applications in light-emitting diodes (LEDs) [14] and high efficiency laser diodes (LDs) [14]. In this Letter, we provide the first experimental observation of current-induced spin polarization in InGaN/GaN superlattices. In addition, we discover that the spin Hall effect can be strongly manipulated by the internal strains. In order to have a fundamental understanding of the strain-induced spin Hall effect, a theoretical investigation has also been performed. Because strains are commonly present in semiconductor multilayers and superlattices due to lattice mismatch, our result therefore provides a convenient way to control the magnitude of the spin Hall effect, which should be very useful for the future applications. Furthermore, this strain dependence enables to resolve the intensive debate about whether the intrinsic spin Hall effect remains valid beyond the ballistic transport regime.

The n-type InGaN/GaN superlattices were grown by a horizontal flow metalorganic chemical vapor deposition on (0001) sapphire substrate. All structures consist of 30 nm buffer layer, followed by a 2 μm epitaxial GaN layer and then 50 periods of InGaN/GaN superlattices. Superlattices are composed of periods of alternating 30 Å GaN barriers and 50 Å In$_x$Ga$_{1-x}$N wells with $x \sim 0.15$. The superlattice was doped with Si, and the electron concentration is 2×10^{12} cm^{-2} according to the Hall measurement. For the cross sectional photoluminescence (PL) measurement, the sample was excited by a He-Cd laser working at 325 nm, dispersed by a SPEX 0.85 m double-grating spectrometer, and the spectra were detected by a photomultiplier tube. Figure 1 shows the experimental arrangement for measuring the current-induced spin polarization. The current flow was stabilized with a value of 80 mA. The laser light was incident along the c axis, which in turn was normal to the growth surface, and the polarized PL spectra were collected along the edge direction of the sample. The cross sectional PL spectra with right-handed (σ^+) and left-handed (σ^-) modes were analyzed with a $\lambda/4$ wave plate and linear polarizer. For applying an electric field, Ohmic contacts were formed by depositing indium drops and a constant current was applied by Keithley 236 source measure unit.

Figure 2(a) shows the cross sectional PL spectra with σ^+ and σ^- polarizations of the InGaN/GaN superlattices without current flow. The main PL signal originates from the recombination of electron-hole pairs in the quantum wells, and the weak modulation on the spectrum is due to the interference effect [15]. The PL spectra were carefully checked by recording zero difference between PL$_{\sigma^+}$ and PL$_{\sigma^-}$ spectra when no current was delivered through the sample. Figures 2(b) shows the intensity variation of the cross sectional PL spectra at 13 K with different orientation of polarization when the current flow is turned on. Here, the angle of 0 degrees is defined as the polarization is
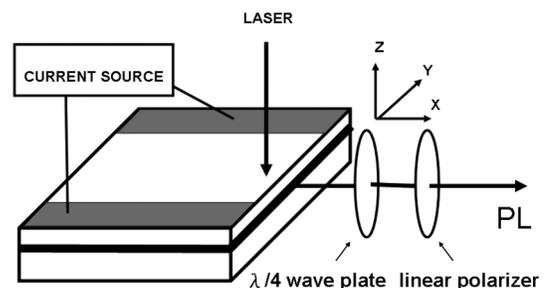

FIG. 1. The schematic diagram of the edge photoluminescence measurement with different angle of polarizer.
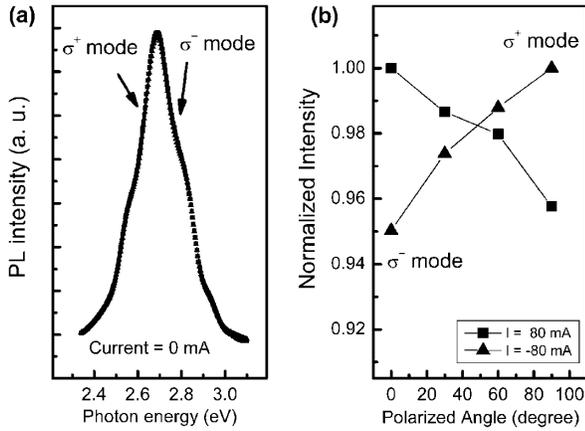
(a)

(b)

FIG. 2. (a) Cross sectional photoluminescence spectra with σ^+ and σ^- polarizations of the InGaN/GaN superlattices in absence of a current. (b) shows the intensity variation of the cross sectional PL spectra with different orientation of polarization when the current flow ($I = +/ - 80$ mA) is turned on at 13 K.

parallel to the c axis of the sample. As can be seen in Figs. 2(b), it reveals a dramatic change in the PL intensity with respect to the polarized angle when the current flow is turned on. With the positive current flow (along the y direction), the PL signal of the σ^- polarization is dominant as compared to that of the σ^+ polarization. On the other hand, the σ^+ polarization PL intensity is dominant for the negative current flow (along the $-y$ direction); i.e., the PL polarization is inverted.

To illustrate the effect of the current flow on the PL spectra in more detail, the difference of the PL intensity between σ^+ and σ^- polarizations is shown in Fig. 3. The base line (dotted line) is taken with the current turned off. The result seems containing a large fluctuations, which may arise from the effect of scattering due to a large defect density existing in nitride semiconductors [6]. Even with the large fluctuations, it reveals an important feature that the difference of the edge PL spectra inverses its sign as the electric current is reversed. In other words, the PL polar-
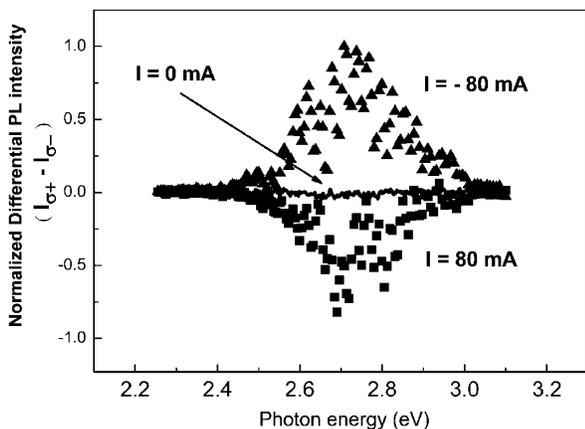

FIG. 3. Differential spectra of polarized photoluminescence. Base line is taken with the current turned off.

ization is inverted as the direction of the current flow is reversed. This is a direct evidence of the current-induced spin orientation, in complete agreement with the results on the spin photocurrents in previous reports [6,7]. It is also worth noting that we did not detect a measurable anisotropy for the in-plane PL spectra with the current flow, and there is also no measurable anisotropy in the edge PL spectrum for the band to band emission when the current is turned off. Thus, the optical anisotropy is a unique property related to the current-induced spin polarization. In addition, to further confirm that the detected optical anisotropy is indeed due to nonequilibrium spin accumulation at sample edges, we have performed and found that the PL polarization is opposite for the two edges.

Let us now briefly outline the underlying mechanism that the nonzero differential edge polarized PL spectra detected in the absence of an external magnetic field is indeed an experimental demonstration of the spin-polarization effect caused by asymmetric band occupation due to the current flow [16]. When a σ-spin electron in the **k** state of the conduction band makes a radiative transition to the topmost heavy-hole subband, the probability of this process depends on σ because the population of hole at the **k** state in the split up subband may be different from that in the split down subband. Hence, at **k** the conduction-band electron spin will be polarized along the σ direction if an electron with (σ) spin has a higher recombination rate. However, since the hole spin orientation at $-$**k** is reversed with respect to that at **k**, the spin polarization of the conduction-band electron at the $-$**k** state will be along the $-\sigma$ direction. Consequently, if the momentum distributions of both the electron gas and the hole gas are isotropic, there will be no net spin polarization of the conduction-band electrons. On the other hand, if such momentum distributions are anisotropic, the generation of spin polarization becomes possible.

To further elucidate the unique behaviors of the spin Hall effect in the InGaN/GaN superlattices, we have measured the edge polarized PL spectra under different excitation power as shown in Fig. 4. We can clearly see that the degree of circular polarization P decreases with increasing pumping power, where P is defined as

$$P = \frac{I_{\sigma+} - I_{\sigma-}}{I_{\sigma+} + I_{\sigma-}}. \tag{1}$$

This interesting result is quite subtle. To understand this intriguing behavior, let us recall the reported photoelastic effect in InGaN/GaN multiple quantum wells [15]. It has been shown that increasing excitation intensity will enhance the screening of piezoelectric (PZ) field due to spatial separation of photoexcited electrons and holes. At the first glance, it seems clear that our observation can be simply explained in terms of the reduced Rashba effect due to the screened electric field. However, one has to keep in mind that nitride semiconductors are excellent piezoelectric materials. Through the converse PZ effect, a change in
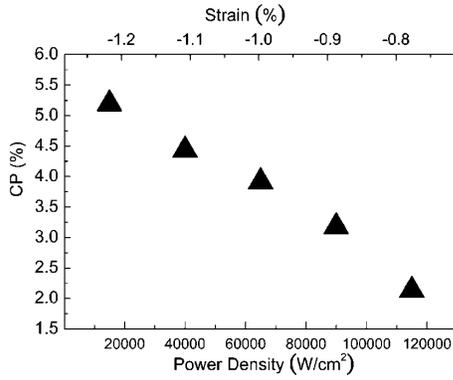
FIG. 4. The degree of circular polarization as a function of
excitation density and corresponding strain. The strain is calcu-
lated by the Raman spectra in Fig. 5. The in-plane electric field is
applied in $-y$ direction.

the built-in electric field can induce a sizable change in the
strain. According to the previous study [11,17], a small
change of strain can have a significant influence on the
Rashba effect, which has been considered as one of the
main causes for the spin Hall effect [1–5]. Therefore, to
complete our understanding, it will be worthwhile to take
the strain effect into account. In order to demonstrate that
the pumping laser can indeed change the internal strain in
the studied sample, we have measured the Raman scatter-
ing of the InGaN/GaN superlattices under different exci-
tation density as shown in Fig. 5. It clearly indicates that
the phonon frequency decreases with increasing pumping
power, which implies that the internal strain of the hetero-
structure due to lattice mismatch can be changed by exter-
nal excitation. The redshift in Raman spectra is unlikely
due to local heating of the sample, because the correspond-
ing PL peak has a blueshift instead of a redshift (not shown
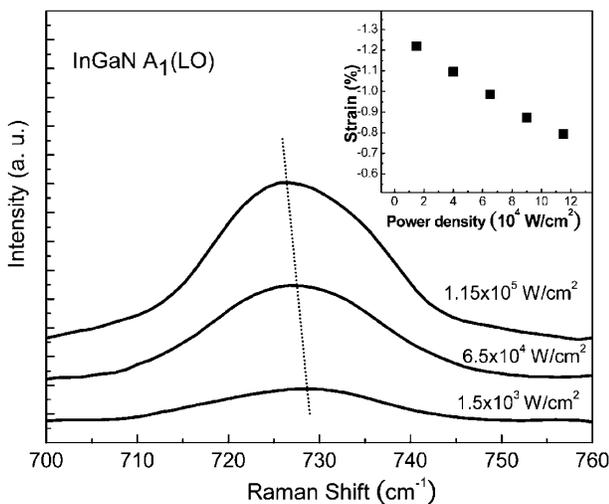

FIG. 5. Raman shift as a function of excitation density. In the
inset, the calculated strain as a function of excitation density. It
shows that the internal strain in InGaN/GaN superlattices can be
manipulated by external excitation.

here). If local heating is significant, the band gap will be
shrunk, which will result in a redshift of the PL spectra. In
addition, the fact that the PL peak of GaN layer remains
unchanged further supports a negligible heating effect. The
strain ϵ change can be calculated according to phonon shift
$\Delta\omega$ by the expression [18]

$$\epsilon = \frac{\Delta\omega}{2a - 2b\frac{C_{13}}{C_{33}}}, \qquad (2)$$

where a and b are phonon deformation potentials, and C_{13}
and C_{33} are the elastic constants, respectively. The calcu-
lated strain is shown in the inset of Fig. 5, where the
deformation potentials a, b and the elastic constants C_{13},
C_{33} were estimated by the extrapolation of the data for
GaN and InN [18].

To establish the fundamental background of the strain-
dependent spin Hall effect in InGaN/GaN superlattices, a
theoretical investigation of the spin Hall current in n-type
two-dimensional (2D) wurtzite structure is performed.
Taking into account of the strong polarization field at the
interface alone the c axis of wurtzite structure and the bulk
inversion asymmetry (BIA), the 2D Hamiltonian can be
written as [19]

$$H = \frac{\hbar k^2}{2m} + (\alpha_e + \beta k^2)(\sigma_x k_y - \sigma_y k_x), \qquad (3)$$

where $\alpha_e = \lambda + \alpha$ is the effective Rashba coupling. The
coupling λ is induced by the built-in electric field due to
the piezoelectric effect. The coupling α and β are due to
the BIA effect. To estimate the coupling parameters α_e and
β, we have performed *ab initio* relativistic band structure
calculations for GaN under several compressive in-plane
strains (0 to -2.0%) using the highly accurate all-electron
full-potential linearized augmented plane wave (FLAPW)
method [20]. The details of the calculations will be re-
ported elsewhere [21]. By fitting the 2D Hamiltonian
[Eq. (3)] to the calculated spin-orbit coupling splitting of
the lowest conduction bands near $k = 0$ as a function of the
wave vector k_x, we obtain the theoretical α_e and β, as
shown in Fig. 6(a) as a function of the in-plane strain. We
note that the theoretical α_e values are in the same order of
magnitude of the effective Rashba coupling measured on
AlGaN/GaN [22]. Since the magnitude of the in-plane
strain in InGaN/GaN is close to that in AlGaN/GaN, the
magnitude of built-in electric field is found to be in the
same order of magnitude in both systems (~ 1 MV/cm)
[23]. Therefore, we may expect InGaN/GaN and
AlGaN/GaN to have similar coupling parameters α_e and
β, and hence the theoretical α_e and β [Fig. 6(a)] will be
used in the following spin Hall conductivity calculations.

Within the linear-response Kubo formalism (see, e.g.,
[24]), we find that the spin Hall conductivity for the 2D
Hamiltonian of Eq. (3) is given by

$$\sigma_{xy}^{s0} = -\sigma_{yx}^{s0} \approx \frac{e}{8\pi}\left[1 + \frac{2}{3}\alpha_e\beta\left(\frac{2m}{\hbar^2}\right)^2\right], \qquad (4)$$

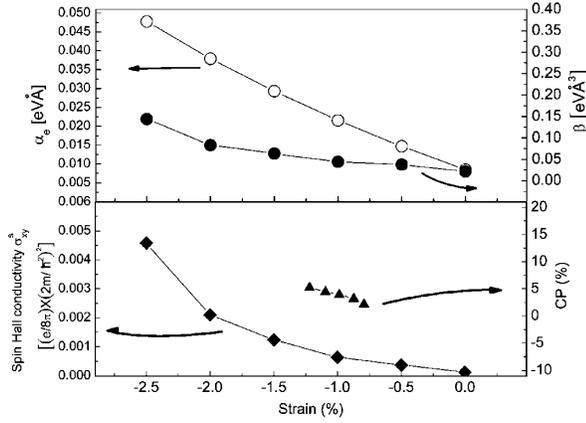FIG. 6. (a) The theoretical effective Rashba coupling $\alpha_e = \lambda + \alpha$ (eV Å) (○) and BIA coupling β (eV Å^3) (●) vs the in-plane strain. (b) The theoretical spin Hall conductivity (σ_{xy}^s) (■) and the degree of circular polarization (CP) (▲) vs the in-plane strain. The in-plane electric field is applied in $-y$ direction.

under the condition that α_e ($\sim 10^{-2}$ eV Å) is larger than $\beta k_{\pm}^2$ ($10^{-3} \sim 10^{-4}$ eV Å), where the k_+ and k_- are the Fermi momenta of the two spin-split bands, respectively. The spin Hall conductivity would be a universal constant, as found before [5], if we set $\beta = 0$. However, it is well known [25] that in the presence of scattering due to, e.g., the disorder, the spin Hall conductivity due to the k-linear coupling term would vanish. Therefore, the observed spin Hall effect would be predominantly due to the k-cubic term, i.e., $\sigma_{xy}^s \approx \frac{e}{8\pi} \frac{2}{3} \left(\frac{2m}{\hbar^2}\right)^2 \alpha_e \beta$. This clearly shows that the spin Hall effect in the wurtzite semiconductor super-lattices and multilayers could be enhanced by manipulating the spin-orbit coupling parameters α_e and β which in term can be tuned by the compressive in-plane strain via the piezoelectric field, as demonstrated by our *ab initio* relativistic band structure calculations [Fig. 6(a)]. The monotonic increase of the calculated spin Hall conductivity as a function of the compressive in-plane strain is in good qualitative agreement with our experimental observation as shown in Fig. 6(b). This correlation implies that the circularly polarized PL spectra observed above are indeed due to the spin accumulation, which can be fine-tuned by the internal strains. We therefore open a new possibility to manipulate the spin Hall effect in semiconductor heterostructures.

In conclusion, we have investigated the current-induced spin polarization in InGaN/GaN superlattices (SLs). It is found that the degree of polarization changes sign as the direction of the current flow is reversed. In addition, we also found that the internal strain in InGaN/GaN super-lattices can be used to manipulate the magnitude of the spin Hall effect. The corresponding theoretical calculation has also been developed to interpret the strain dependence of the spin Hall effect. The strain-induced spin Hall effect discovered here paves an alternative way for the creation of

spin polarized current, which should be useful for the realization of the future applications in spintronics. In view of the wide range of applications in nitride semi-conductors, our study shown here should be very useful and timely.

[1] M. I. Dyakonov and V. I. Perel, Sov. Phys. JETP **33**, 1053 (1971).
[2] S. Datta and B. Das, Appl. Phys. Lett. **56**, 665 (1990).
[3] J. E. Hirsch, Phys. Rev. Lett. **83**, 1834 (1999).
[4] S. D. Ganichev and W. Prettl, J. Phys. C **15**, R935 (2003), and references therein.
[5] J. Sinova, D. Culcer, Q. Niu, N. A. Sinitsyn, T. Jungwirth, and A. H. MacDonald, Phys. Rev. Lett. **92**, 126603 (2004).
[6] Y. K. Kato, R. C. Myers, A. C. Gossard, and D. D. Awschalom, Science **306**, 1910 (2004).
[7] J. Wunderlich, B. Kaestner, J. Sinova, and T. Jungwirth, Phys. Rev. Lett. **94**, 047204 (2005).
[8] S. Murakami, N. Nagaosa, and S.-C. Zhang, Phys. Rev. Lett. **93**, 156804 (2004).
[9] E. I. Rashba, Phys. Rev. B **70**, 201309(R) (2004).
[10] A. A. Burkov, A. S. Nunez, and A. H. MacDonald, Phys. Rev. B **70**, 155308 (2004).
[11] G. Y. Guo, Y. Yao, and Q. Niu, Phys. Rev. Lett. **94**, 226601 (2005).
[12] J. E. Hirsch, Phys. Rev. B **71**, 184521 (2005).
[13] N. P. Stern, S. Ghosh, G. Xiang, M. Zhu, N. Samarth, and D. D. Awschalom, Phys. Rev. Lett. **97**, 126603 (2006).
[14] S. Nakamura and G. Fasol, *The Blue Laser Diode* (Springer, New York, 1997).
[15] T. Y. Lin, Appl. Phys. Lett. **82**, 880 (2003).
[16] A. G. Mal'shukov and K. A. Chao, Phys. Rev. B **65**, 241308(R) (2002).
[17] D. M. Gvozdic and U. Ekenberg, Europhys. Lett. **73**, 927 (2006).
[18] A. G. Kontos, Y. S. Raptis, N. T. Pelekanos, A. Georgakilas, E. Bellet-Amalric, and D. Jalabert, Phys. Rev. B **72**, 155336 (2005), and references therein.
[19] I. Zorkani and E. Kartheuser, Phys. Rev. B **53**, 1871 (1996).
[20] P. Balaha, K. Schwarz, G. Madsen *et al.*, *wien2K, An Augmented Plane Wave Local Orbitals Program for Calculating Crystal Properties* (Technology University Wien, Austria, 2002).
[21] G. Y. Guo *et al.* (to be published).
[22] K. S. Cho, T. Y. Huang, H. S. Wang, M. G. Lin, T. M. Chen, C.-T. Liang, Y. F. Chen, and I. Lo, Appl. Phys. Lett. **86**, 222102 (2005).
[23] N. Grandjean, J. Massies, and M. Leroux, Appl. Phys. Lett. **74**, 2361 (1999).
[24] T.-W. Chen, C.-M. Huang, and G. Y. Guo, Phys. Rev. B **73**, 235309 (2006).
[25] J. Sinova, S. Murakamib, S. Q. Shenc, and M. S. Choi, Solid State Commun. **138**, 214 (2006).